

Double-Sided Rotor Technology for Iron-Cored Permanent Magnet Wind Generators: An Evaluation

Johannes H. van Wijk

Department of Electrical and Electronic Engineering
Stellenbosch University
Stellenbosch, South Africa

Maarten J. Kamper

Department of Electrical and Electronic Engineering
Stellenbosch University
Stellenbosch, South Africa
kamper@sun.ac.za

Abstract—In this article a double-sided rotor technology for an iron-cored permanent magnet direct-drive wind generator is evaluated. The evaluation is based on the finite element and laboratory test results of an optimum designed 15 kW iron-cored permanent magnet wind generator. Aspects such as mass, performance quality, cooling characteristics and efficiency, amongst others inherent in such a study are investigated. Although the double-sided rotor permanent magnet wind generator requires nearly twice the magnetic volume compared to the conventional single-sided permanent magnet wind generator, its active mass turns out to be less than that of both the single-sided rotor generator and an air-cored permanent magnet wind generator of the same power level. The double-sided rotor topology furthermore becomes attractive because of its inherent cooling characteristics, which are evident in its low operating temperatures.

Keywords—double-sided rotor, iron-cored, light-weight, efficiency, permanent magnet, direct-drive wind generator.

I. INTRODUCTION

Even though harnessing wind energy is the cheapest renewable energy technology available today, it still has a cost disadvantage relative to the well-established fossil energy sources. By reducing the number of stages in the power takeoff of a wind turbine system, its reliability increases and so the over-all cost of harnessing this free energy source is reduced. With the growing power demand, the adoption of direct-drive systems is limited, due to their undesirable, yet related, growth in size, weight and cost. As a result, present and future trends in direct-drive wind turbine development focuses on lowering the cost of energy for this sustainable energy source through maximizing the wind energy conversion efficiency and the reliability of these generation systems, while minimizing material usage and hence, mass. The last mentioned are three common goals amongst wind turbine developers aimed at achieving a greater goal, namely cost savings. Therefore, to make wind energy economically feasible means that the power density (power output/active volume) should also be maximized.

Interestingly, Percy H. Thomas, in a study that he

The financial assistance of the South African National Energy Research Institute (SANERI) toward this research is hereby acknowledged. Opinions expressed and conclusions arrived at, are those of the authors and are not necessarily those of SANERI.

performed in the 1940's, concluded that machines in the size range of 6.5 – 7.5 MW were necessary for economic viability [1]. Currently, wind turbines in the size range of 3 - 4.5 MW are widely installed, while the introduction of turbines in the 5 – 6 MW range, such as the M6 (RE Power) and M5000 (AREVA), to the market also takes place.

Conventional permanent magnet (PM) direct-drive machines of this size pose great difficulty and danger during assembly. The strong magnetic pull forces that exist between the single-sided rotor and stator furthermore put a strenuous load on the supporting structures and bearings, often resulting in eccentricity between rotor and stator. Oval formed rotor and/or stator supporting structures are also a result of unbalanced magnetic pull and insufficient structural strength.

Adopting the air-cored methodology for wind turbine generators eliminates all magnetic attraction forces between the rotor and stator and therefore eases their treading [2]. The double-sided rotor topology often accompanies this solution, as is evident in literature [3][4][5]. Eddy currents and poor heat dissipation are some of the challenges air-cored machines pose.

In this article an evaluation of the double-sided rotor technology in iron-cored PM wind generators, is provided.

II. ROTOR TOPOLOGIES

A. Reduction of Field Force Effects

In an attempt to understand the radial attraction forces that exist in direct-drive electrical machines and that demand bulky structural support to maintain the desired air gap clearance, the electromechanical-energy conversion of such machines was investigated in a previous study [6]. Three rotor yoke topologies, those are a single-rotor, a double-rotor and an unconventional C-shaped modular rotor yoke as shown in Figure 1, are compared in order to determine the most

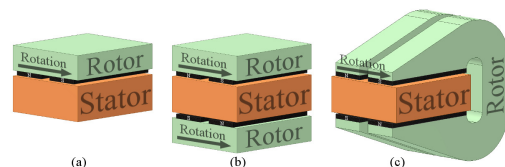


Figure 1. Three Radial Flux Rotor-Stator configurations investigated - (a) Single-rotor, (b) Double-rotor, (c) C-core rotor.

beneficial rotor-stator topology. The aim is to significantly reduce the structural mass of direct-drive iron-cored PM wind turbines by eliminating or at least reducing the unwanted effects of the radial magnetic forces in iron-cored generators.

The single-rotor and double-rotor yoke topologies both have a longitudinal flux path, whereas the C-shaped yokes provide a transverse flux path. The magnetic forces that exist between the rotor and stator consist of two components, namely the shear forces (quantified as torque and required for power generation) and radial forces (responsible for producing radial vibration in and attraction forces between rotor and stator iron parts). In the latter two topologies the radial field forces in the two air gaps will oppose each other, thus theoretically resulting in zero resultant force on the stator if it is positioned with exactly equal air gap clearances on either side.

B. C-cored PM Rotor Machine

The topology with the isolated C-shaped yoke modules provides a flux path whereby the field force in both air gaps is made completely independent of the stator positions as presented in [6], but flux leakage located around the sides of the magnets prohibits the elimination of the attraction forces on the iron-cored stator. None the less, these field force effects on the stator are less than 1%, compared to those in a single-sided rotor PM machine

Interestingly, in the 300 kW PM generator feasibility study [6], the C-shaped rotor yoke topology required less structural material, but utilized 33% more active material compared to an equally sized generator with a single-sided rotor. The C-shaped yokes alone contributed 61% of this mass. Unlike the modular yoke structure of the C-Gen which provides both longitudinal and transverse flux paths [3], this topology does not permit lesser yoke material usage.

C. Single-sided PM Rotor Machine

In a previous study [5], a single-sided iron-cored direct-drive PM wind generator [11] with an outer surface mounted PM rotor and an inner stator, is compared on a 15 kW power level to a double-rotor air-cored wind generator with surface mounted permanent magnets. This single-sided iron-cored PM generator is used as the benchmark for the double-sided iron-cored PM wind generator presented in this paper.

D. Double-sided PM Rotor Machine

Figure 2 shows a cross-section of a double-sided rotor (also referred to as dual-rotor [7] [8]) iron-cored radial flux PM machine. This specific machine has a back-to-back stator configuration which shares a common yoke and employs toroidally wound stator windings.

In such a double-sided rotor design, active material volume and weight is of concern. In a conventional generator with a single-sided rotor, the stator yoke alone contributes to one third of the total active material mass. Air-cored topologies do not pose any advantage for weight reduction, because of the excessive amount of magnetic material required to maintain the same power level [5].

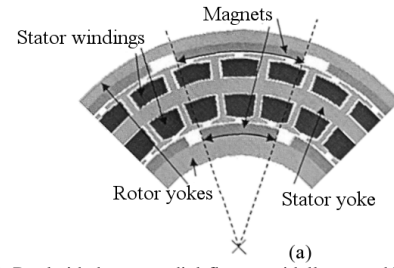


Figure 3. Dual-sided rotor, radial-flux, toroidally wound PM machine

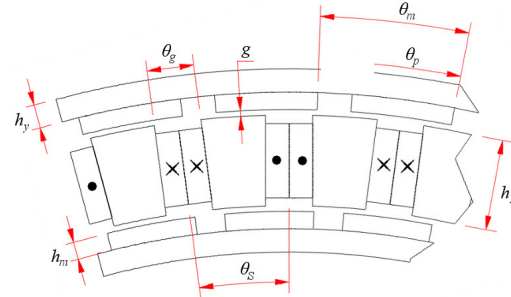


Figure 2. Section of the double-sided rotor PMSG model.

In the study presented in this paper an iron-cored wind generator with a double-sided rotor topology, is investigated. The weight concern is addressed by introducing a yokeless stator design as shown in Figure 3. This design has inherent modular manufacturing advantages.

III. ELECTRICAL DESIGN OPTIMIZATION

The average electromagnetic developed torque of a concentrated winding PM machine can be expressed by [9]

$$T_{ave} = 1/4 k_w n_l n_t Q_s B_{\delta 10} A_\delta I \cos(\theta), \quad (1)$$

where k_w is the fundamental winding factor, n_l is the number of layers (single or double), n_t is the number of tooth turns, Q_s is the number of slots, is the peak value of the fundamental no-load air gap flux density, A_δ is the air gap area, I is the peak value of the phase current and θ is the current angle. It is therefore advantageous to find a good winding factor, which is greatly determined by the pole-slot combination.

The induced EMF in the stator winding is investigated in order to determine the winding factor for various possible pole-slot combinations, as explained in [10]. At an operating frequency of 50 Hz and at a speed of 150 r/min, the pole number will be 40. This allows the double-sided rotor machine under investigation to be compared with the single-sided rotor machine in [5] and [10].

From Table I a pole-slot combination of 40-48 gives an acceptable winding factor of 0.933, while a winding section of $W_s = 8$ is obtained, which allows for smaller stator modules and faster finite element (FE) simulation times. The performance parameters of the generator are given by U and the dimensional variables in Figure 3 are given by X. The magnet pitch, σ_m and slot pitch, σ_s are represented as a fraction of the pole pitch, θ_p and slot pitch, θ_s as shown in Figure 3.

TABLE I. POSSIBLE SLOT NUMBERS FOR A 40 POLE MACHINE

| $P = 40$ | Q_s | 30 | 36 | 42 | 45 | 48 | 54 |
|----------|-------|-------|-------|-------|-------|-------|-------|
| | q | 1/4 | 3/10 | 7/20 | 3/8 | 2/5 | 9/20 |
| | k_w | 0.866 | 0.945 | 0.953 | 0.945 | 0.933 | 0.877 |
| | w_s | 10 | 4 | 2 | 5 | 8 | 2 |

$$\mathbf{U} = \begin{bmatrix} P_0 \\ n_s \\ f \end{bmatrix} = \begin{bmatrix} 15 \text{ kW} \\ 150 \text{ r/min} \\ 50 \text{ Hz} \end{bmatrix} \quad (2)$$

$$\mathbf{X} = [h_y \ h_m \ h_s \ \sigma_m \ \sigma_g]^T \quad (3)$$

The optimization method followed minimizes the active mass of the machine by varying its five dimensional parameters, whilst ensuring that the average required developed torque of 1000 Nm is maintained. This gives a near optimum value from each machine parameter. Keeping h_y , h_m and h_s fixed, σ_m and σ_g are varied in small increments to minimize load torque ripple.

Closing the slot opening by nearly 50% and skewing the two rotors relative to each other, as shown in Figure 4, reduced the load torque ripple further. In Figure 5 the effect of skewing on the developed torque in one air gap relative to the other, i.e. aligning the peaks of the one ripple waveform with the valleys of the other and vice versa, is shown.

IV. ROTOR CONSTRUCTION DESIGN

The mechanical design of the double-sided rotor PM generator is aimed at simplifying the assembling process, while still maintaining the required precise placement of the different machine components.

A. Yoke Height

The yoke height, h_y , is determined by the electro-magnetic requirements of the machine. During the mechanical FE evaluation, the structural rigidity of the rotor structure was found to be more than sufficient to withstand the magnetic attraction forces in the air gap and ensure that the designed air gap clearance is maintained during operating and non-operating conditions. The operational magnetic attraction forces acting on each of the two rotor yokes are obtained from the electro-magnetic FE analysis, and are used in the mechanical strength calculations. Figure 6 shows the expected deformation of the inner rotor yoke. Figure 7 shows the rotor support studs mounted on the rotor plate and the completed yokes.

B. Yoke Support

The studded rotor yoke support structure selected for the prototype generator offers various advantages over that of the solid support frame. For one, air flows freely over the backs of both rotor yokes and through the air gaps between rotor and stator, which enhance the dissipation of heat caused by iron losses in the yokes. Turbulent air flow created by the surface mounted magnets enhances the cool-hot air exchange over the stator cores with a positive effect on the machine's losses.

Much less material is needed for the support frame of the rotor yokes, promising a light weight structure. The

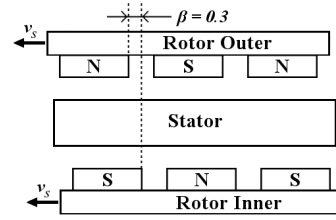


Figure 4. Schematic of skewed double-sided rotor.

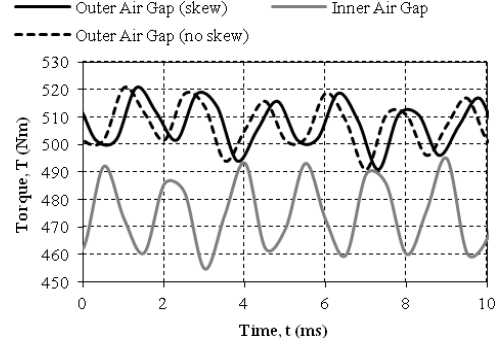


Figure 5. Minimizing effect on load torque ripple through rotor skewing.

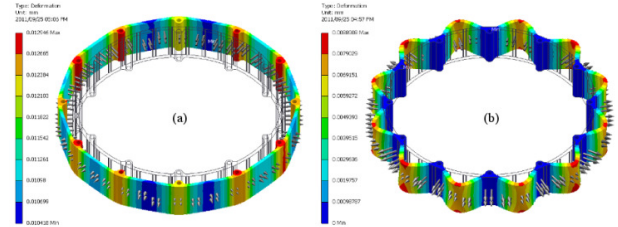


Figure 6. Deformation of inner rotor yoke with (a) no constraint and (b) fixed constraints.

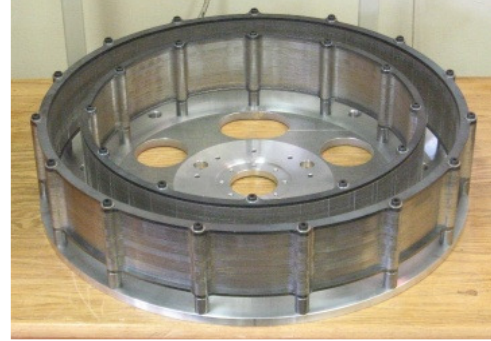


Figure 7. Completed rotor yokes mounted on rotor plate.

manufacturing of the studs is also less laborious and much cheaper than that of the solid frame.

The number of studs and their design are determined by the steady state torque and the fluctuating loads they are required to carry, and are validated by mechanical FE software.

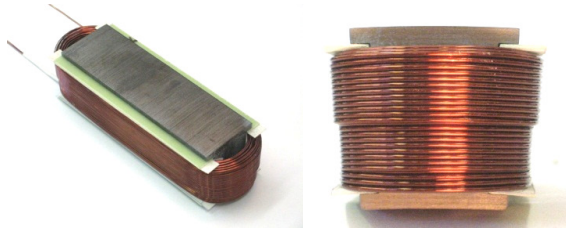


Figure 8. Completed cored coil module.

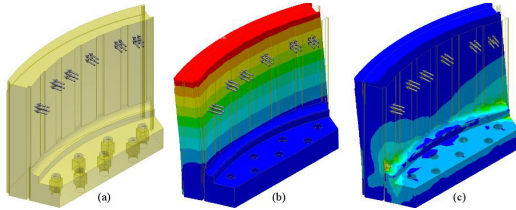


Figure 9. Prediction of stator segment deformation and stress concentrations.

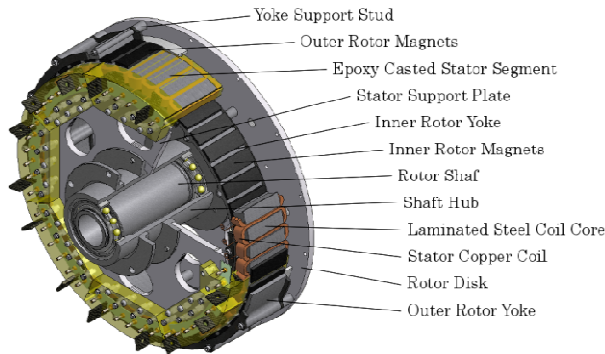


Figure 10. A CAD illustration of the double-sided rotor PMSG.

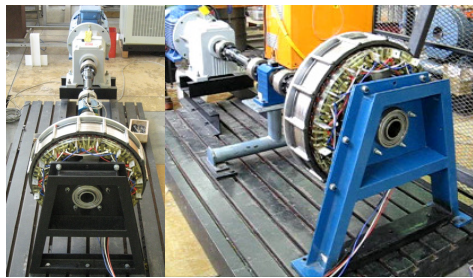


Figure 11. Built prototype PMSG on test bench.

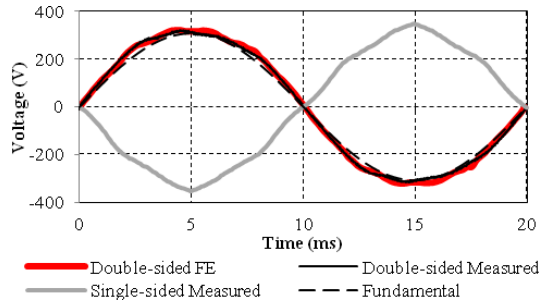


Figure 13. FE-calculated and measured open circuit induced voltages at rated speed.

V. STATOR CONSTRUCTION DESIGN

The non-overlap double-layer winding configuration selected for the yokeless stator design allows for the copper wire to be wound directly onto a laminated stator coil core to form the stator coil module shown in Figure 8. Six of these coil modules are cast epoxy resin to form a stator module/segment.

The mould used for the stator module casting, is designed to give the stator casting a final form that will keep stress concentration within acceptable limits and that will ensure precise placement/positioning of the coil cores. Figure 9 shows the FE model and its deflection and stress concentration results. The sides of the stator modules are also provided with a profile that slots into the adjacent segments and guides the insertion into and recovery from the machine.

VI. PROTOTYPE EVALUATION

The double-sided rotor PM prototype generator of Figure 10 was built and tested. The test system is shown in Figure 11. The test results obtained are compared to those from the FE evaluation and those of the single-sided rotor test results presented in [5].

A. Voltage Quality

The induced open circuit voltage waveform results are shown in Figure 12. The induced voltage quality of the double-sided rotor PM generator, with its double layer non-overlap winding, seems to have a more sinusoidal waveform in the time domain and at rated speed, compared to that of the single-sided PM generator at the same operating conditions.

Considering the harmonic content of both machines it is interesting to note the eminent 3rd harmonic of the double-sided rotor machine in Figure 13. As third harmonic induced three-phase voltages are co-phasor, no third harmonic three-phase currents will flow in the wye stator connection, as is also clear from the current waveform in Figure 14. For the first 40 harmonics the total harmonic distortion (THD) of the induced voltage is calculated by [4]

$$THD_V(\%) = \frac{\sqrt{\sum_{n=2}^{\infty} V_n^2}}{V_1} \quad (4)$$

where V_n is the voltage amplitude of the n^{th} order harmonic frequency and V_1 is the voltage amplitude of the fundamental frequency. The THD_V is calculated to be 5.72%, compared to the 4.29% THD_V of the single-sided rotor PM generator, which clearly shows the distorting effect of the dominant 3rd

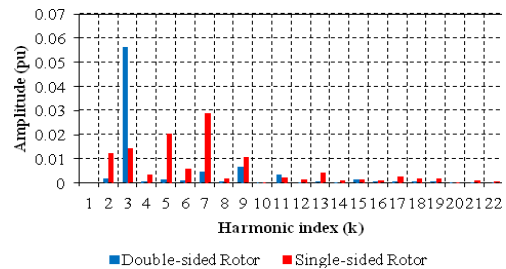


Figure 12. Amplitudes of the harmonics present in the no-load voltage waveform.

harmonic. The THD of the rated load voltage and currents are calculated to be 5.42% and 0.83% respectively.

B. Torque Quality

Two machine parameters in wind generators, that quantify the quality of the machine's torque, are torque ripple and cogging torque. It is evident from [11] that the slightest change

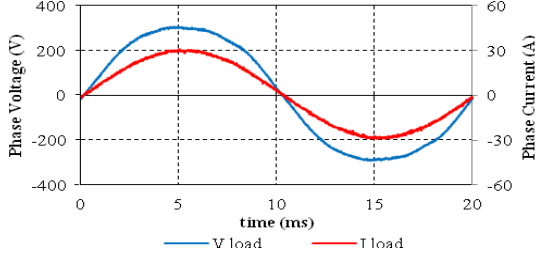


Figure 14. Phase voltage and current measured at rated speed with a resistive load.

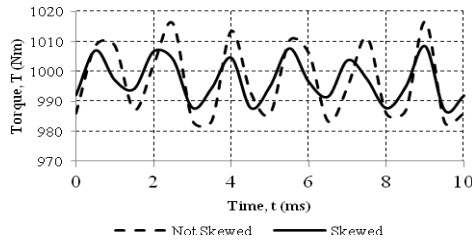


Figure 15. Minimizing effect on load torque ripple through rotor skewing.

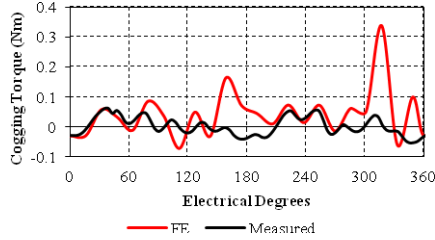


Figure 16. Cogging torque simulated and measured results.

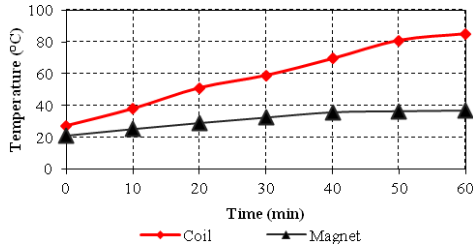


Figure 17. Temperature rise during a full resistive load test at rated speed.

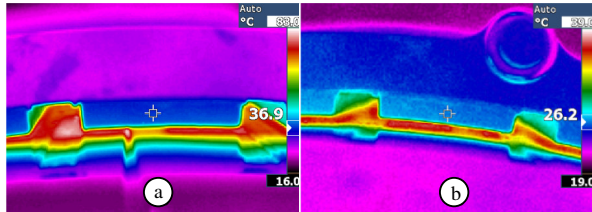


Figure 18. Thermal image for (a) a magnet after operating at rated with a full resistive load and (b) magnet after a short-circuit test.

in the dimensional parameter of an electrical machine, significantly affects its torque ripple. This outcome is used advantageously to improve the torque ripple of the double-sided rotor PM generator with minor changes to its average torque, as shown in Figure 15.

Dynamic effects contained within the drive train of the test setup made it impossible to accurately measure the cogging torque in a dynamic test. A static cogging torque test setup, as proposed in [11], is thus used. Test results showed a significant cogging torque value of 11% relative to the rated torque. This value is lower and more consistent over the full electrical degree range than that of the FE predicted value of 17%, as can be seen in Figure 16.

C. Temperature Rise and Cooling

All tests were performed in a laboratory with an ambient temperature of about 20 °C and no air flow, thus the magnet and coil temperatures are expected to be higher than in real wind turbine applications with sufficient air flow to replace hot air near the active component surfaces with cooler air.

Temperature monitoring was performed during two tests: first a 60 minute continuous operating period at rated speed and with a full resistive load, and second a short-circuit test. Figure 17 shows the captured component temperatures during the resistive load test. The magnet temperature seems to have stabilized after the 60-minutes, while the temperature curve of the stator coil cores also show that it is reaching a stabilization value. Figure 18 shows the thermal images taken of the final stator coil core and magnet temperatures.

A very small effect on the temperature of the magnets and coil cores is noticed during the short circuit test, which was performed after the resistive load tests. The thermal images of Figure 18 once again show low final temperatures, proving the excellent inherent cooling property of the design.

The relatively low operating temperatures of the double-sided rotor PM generator are mostly due to the mechanical design and construction of the machine, which allows for sufficient air flow through the two air gap clearances. The yokeless stator design in effect doubles the surface area through which the heat exchange takes place. The surface mounted PMs create turbulent air flow over these surfaces, and this enhances the machine's cooling ability further:

D. Efficiency

Figure 19 shows the measured input power and output power of the generator over the full range of operating speed and with a full-load resistive load. It is interesting to note the high efficiency of the double-sided rotor PM generator when compared to the efficiencies of the air-cored and iron-cored PM generators in [5], which are 92.6% and 93.5% respectively.

VII. CONCLUSION

In this study a double-sided rotor iron-cored PM generator is designed, built and tested with satisfactory results.

Two important contributors to the light weight attribute of the double-sided rotor topology are the yokeless stator and the

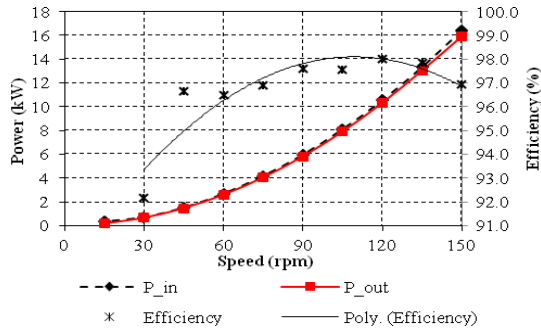


Figure 19. Efficiency of the double-sided rotor PMSG with full resistive load.

studded rotor yoke support structure. Both these attributes can be introduced to other topologies for weight reduction.

An important advantage of the yokeless stator design is that it allows for the copper wire to be wound directly onto the stator coil cores, giving it a good slot fill factor of 0.53. The double-layer stator winding configuration selected for this design, also allows for shorter end windings and a smaller stator height, which reduces the active material mass even further. Another significant advantage of the yokeless stator is its inherent large stator-air interface, which enhances the heat exchange rate.

With a yokeless stator, it is possible to manufacture iron cored coil modules and group them to form modular stator sections. This holds great advantages since a smaller (and cheaper) mould is required for casting the modular stator sections. Handling and assembling of rotor and stator are, thus, also simplified. A modular stator furthermore allows for easy and quick replacement of faulty stator sections with off the shelf units which will reduce generator down time significantly.

TABLE II. DESIGN RESULTS OF DOUBLE-SIDED ROTOR PMSG

| Parameters | Three 15 kW PMSGs | | |
|--|-------------------|---------|---------|
| | SSR ICS | DSR ICS | DSR ACS |
| Outer diameter (mm) | 653.5 | 653.5 | 678 |
| Inner diameter (mm) | 494 | 520.34 | 576 |
| Active axial length (mm) | 100 | 100 | 149 |
| Magnet height (mm) | 6 | 6.32 | 9.7 |
| Stator (slot) height (mm) | 53 | 33 | 11.42 |
| Copper mass (kg) | 23.9 | 14.3 | 15.5 |
| Active iron mass (kg) | 58.9 | 55.3 | 43.9 |
| Magnetic material mass (kg) | 6.5 | 13.7 | 30.1 |
| Total active mass (kg) | 89.4 | 83.2 | 89.5 |
| Structural + active mass (kg) | 174 | 160 | 164.4 |
| Synchronous reactance (p.u.) | 0.471 | 0.103* | 0.063 |
| Phase resistance (p.u.) | 0.034 | 0.035 | 0.072 |
| Current density (A/mm ²) | 3.39 | 4.71 | 6.0 |
| Power factor {I _d = 0A} | 0.934 | 0.999 | 0.998 |
| Efficiency {I _d = 0A} | 93.5 | 96.7 | 92.6 |
| Copper losses (W) | 749 | 574 | 1124 |
| Stator eddy current losses (W) | - | - | 34.4 |
| Stator iron losses (W) | 246 | 110 | - |
| Stator loss/stator volume (kW/m ³) | 90 | 112 | 345 |

* Value obtained from FE calculations – The real synchronous reactance is anticipated to be higher, but still much lower than that of the single-sided rotor PMSG's reactance value.

The performance qualities of the voltage and current waveforms of the double-sided rotor iron-cored PM generator are within acceptable limits. The undesired and relatively high cogging torque of the prototype is not the result of irregular stator coil placement, non-uniform air gap length in the machine or any other mechanical discrepancies. Its cause needs further investigation to ensure easy start-up and to make it feasible for direct-drive wind turbine applications. This study has, however, shown that the proposed topology is a very good choice for obtaining a highly efficient generator.

In this study the double-sided rotor PM generator (DSR ICS) is found to be lighter than both the single-sided iron-cored PM generator (SSR ICS) and the double-sided rotor air-cored PM generator (DSR ACS). Design results and comparisons are tabulated in Table II. There is, therefore, no reason why a double-sided iron-cored PM machine with a yokeless stator should be heavier than other topologies.

VIII. REFERENCES

- [1] G.L. Johnson, "Wind energy systems", published by Prentice-Hall Inc., Englewood, Cliffs, NJ, 1985.
- [2] M.A. Meuller, A.S. McDonald, "A lightweight low speed permanent magnet electrical generator for direct drive wind turbines", EWEC, Brussels, 2008
- [3] N. Hodgins, A. McDonald, J. Shek, O. Keysan and M. Mueller, "Current and future development of the C-Gen lightweight direct drive generator for wave and tidal energy", European Wave and Tidal Energy Conference, pp. 352-359, Uppsala, Sweden, 7-10 September 2009
- [4] J.A. Stegmann and M.J. Kamper, "Design Aspects of Double-sided Rotor Radial Flux Air-Cored Permanent-Magnet Wind Generator" IEEE Transaction on Industrial Applications, vol.47, no.2, pp.767-776, March/Apr 2011.
- [5] M.J. Kamper, J.H.J. Potgieter, J.A. Stegmann and P. Bouwer, "Comparison of Air-Cored and Iron-Cored Non-Overlap Winding Radial Flux Permanent Magnet Direct Drive Wind Generators", IEEE Energy Conversion Congress & Expo (ECCE, Phoenix, Arizona, Sept. 18-22, 2011
- [6] J.H. van Wijk, M.J. Kamper, "C - core topology for PM wind generators with non-overlap iron-cored stator windings ", in IET Int. Conf. Power Electron., Mach. and Drives, Brighon, 2010, p. 6
- [7] R. Qu, T.A. Lipo, "Dual-rotor, radial-flux, toroidally-wound, permanent-magnet machines", IEEE-IAS Conf. Rec. Pittsburgh, PA, Oct 2002, vol. 2, pp. 1281 - 1288
- [8] R. Qu, M. Aydin, T.A. Lipo, "Performance Comparison of Dual-Rotor Radial-Flux and Axial-Flux Permanent-Magnet BLDC Machines", Proc. Electric Machines and Drives Conference (IEMDC'03), IEEE International, 1-4 June 2003, Vol. 3, pp. 1948 – 1954.
- [9] F. Magnussen, C. Sadarangani, "Winding Factors and Joule Losses of Permanent Magnet Machines with Concentrated Windings", Electric Machines and Drives Conference (IEMDC'03), vol. 1, pp. 333 – 339, June, 2003.
- [10] F. Liber, J. Soulard, "Investigation on Pole-Slot Combinations for Permanent-Magnet Machines with Concentrated Windings", Proc. of Int. Conf. on Electrical Machines (ICEM'04), Cracow, Poland, 5-8 September 2004.
- [11] J.H.J. Potgieter, M.J. Kamper, "Cogging Torque Sensitivity in Design Optimisation of Low Cost Non-Overlap Winding PM Wind Generator", Int. Conf. on Electrical Machines (ICEM'10), Rome, Italy, Sept. 2010.
- [12] R. Qu, T.A. Lipo, "Dual-rotor, radial-flux, toroidally-wound, permanent-magnet machines", IEEE-IAS Conf. Rec. Pittsburgh, PA, Oct 2002, vol. 2, pp. 1281 - 1288
- [13] R. Qu, M. Aydin, T.A. Lipo, "Performance Comparison of Dual-Rotor Radial-Flux and Axial-Flux Permanent-Magnet BLDC Machines", Proc. Electric Machines and Drives Conference (IEMDC'03), IEEE International, 1-4 June 2003, Vol. 3, pp. 1948 – 1954.